EFFECT OF UPGRADING WFP CONNECTION WITH DOUBLE-I-SECTION COLUMN USING SIDEPLATE-WITH-OPENING ON FRAME PERFORMANCE

A. Deylami[1] and M. Nazokkarmaher[2]

[1] *Ardeshir Deylami, Assistant Professor, Department of Civil and Environmental Engineering, Amirkabir University of Technology, Tehran, Iran (E-mail: deylami@aut.ac.ir)*
[2] *Moosa Nazokkarmaher, M.Sc Student, Department of Civil and Environmental Engineering, Amirkabir University of Technology, Tehran, Iran (E-mail: moosamaher@aut.ac.ir)*

ABSTRACT :

The objective of this paper is to evaluation of frame performance with WFP connections and double-I-section column and compares it with the upgraded performance of frame when the connections are retrofitted with Sideplate-with-Opening. So 3, 7 and 12 story frame are designed with the both existing and upgraded connections. Typically 20 connections with different beam and column size are designed. 6 connections were selected for finite element study. Moment-rotation of connection, panelzone and rotational capacity of the selected connections are extracted using finite element method. Parametric studies are performed to develop equation for prediction of remaining 14 connections behavior. Frame performance level is calculated based on interstory drift to connection rotational capacity. Frame response is calculated with nonlinear time history analysis under 7 known earthquake. Connections and panelzones are modeled with multilinear and linear springs, respectively.

KEYWORDS :

WFP; Double-I-section; Sideplate-with-Opening; Parametric study; Finite element; Frame Performance.

1. INTRODUCTION

WFP connection is such postnorthrige connections. The qualifying cyclic test of this connection is preformed on wide flange columns. Because of lack of wide flange sections in Iran in the most cases double-I-section columns are used with WFP connections. However, researches show that WFP connection has PR and brittle behavior when it is used with box-shaped column. Double-I-section columns significantly have box-shaped characteristics. PR and brittle behavior cause to increase frame drift and decrease connection rotational capacity. So it has inverse effect on frame performance. This type of connection is shown in Figure 1.

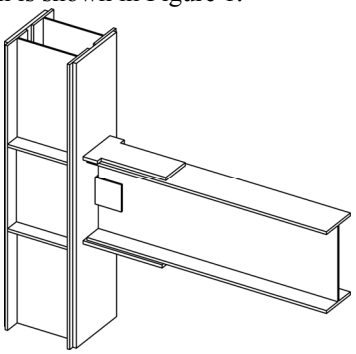

Figure 1: Typical existing WFP connection with double-I-section column

This article recommends Sideplate-with-Opening (SPO) in order to improve the behavior of the existing WFP connections with double-I-section columns. Upgrading WFP connection using SPO modifies the force transmission mechanism so the connection behavior improves considerably that cause to enhance frame performance. Typical upgraded connection is shown in Figure 2.

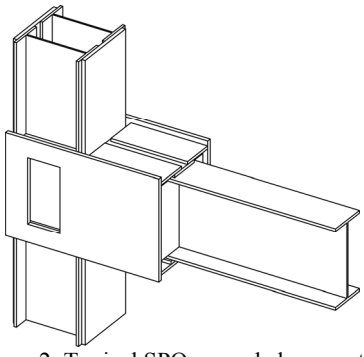

Figure 2: Typical SPO upgraded connection

The new upgrading elements are added to existing connection. Opening is considered in sideplate that the orthogonal beam could passes through. The new flange cover plates are used to fill the differences between sideplates and existing flange plates. Top cover plate is implemented in two pieces in order to welding in flat

position. All new welds are fillet welds and existing welds are left in place.

2. Frames and Connections

Three 3, 7 and 12 moment frame are designed according to common design procedure in Iran with WFP connections with double-I-section columns. All story's height are 3m and all bay's width are 5m. Gravity loads are the same for frames. Beams and columns are designed based on equivalent load procedure in standard 2800 [1] assuming that connections are rigid and frame is SMF type. Designed frame are shown in Figure 3. Details of designed double-I-section columns are presented in Figure 4 and Table 1.

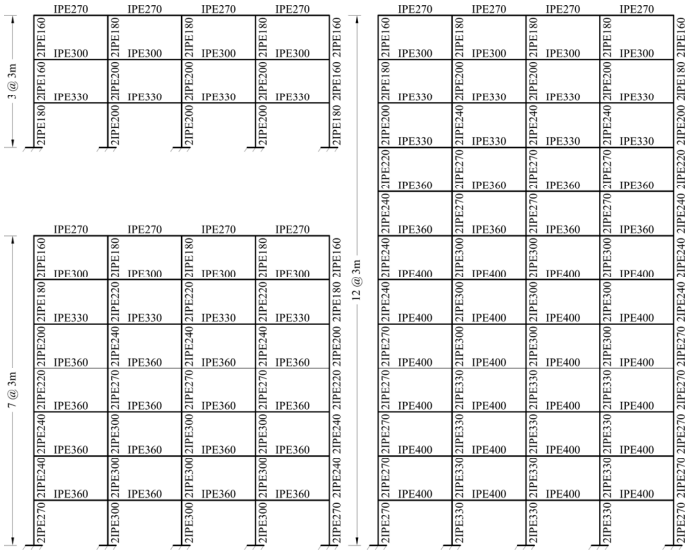

Figure 3: Designed frames assuming rigid connections

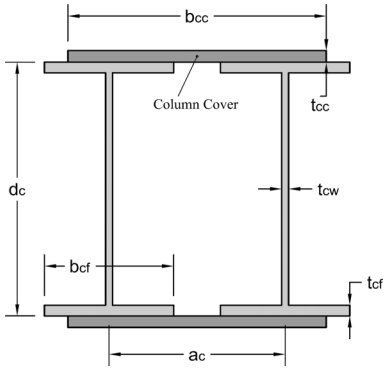

Figure 4: Double-I-section column details

Table 1: Double-I-section column detail

Column Section	Column I-section				Column Cover		I-section distance
	d_c	b_{cf}	t_{cf}	t_{cw}	b_{cc}	t_{cc}	a_c
2IPE160	16	8.2	0.74	0.5	16	0.8	11
2IPE180	18	9.1	0.8	0.53	18	0.8	12
2IPE200	20	10	0.85	0.56	20	1	14
2IPE220	22	11	0.92	0.59	22	1	15
2IPE240	24	12	0.98	0.62	24	1	16
2IPE270	27	13.5	1.02	0.66	27	1.5	17.5
2IPE300	30	15	1.07	0.71	30	1.5	19
2IPE330	33	16	1.15	0.75	33	2	21

- all dimensions: cm

Existing WFP connections are designed according to seismic provision of standard 2800 [1] assuming SMF connections. Details of designed existing connections are presented in Figure 5 and Table 2.

Upgrading SPO elements are designed based on capacity method. In this method new elements are designed for capability of transferring strength forces of existing element. Details of designed Upgrading elements are presented in Figure 6 and Table 3.

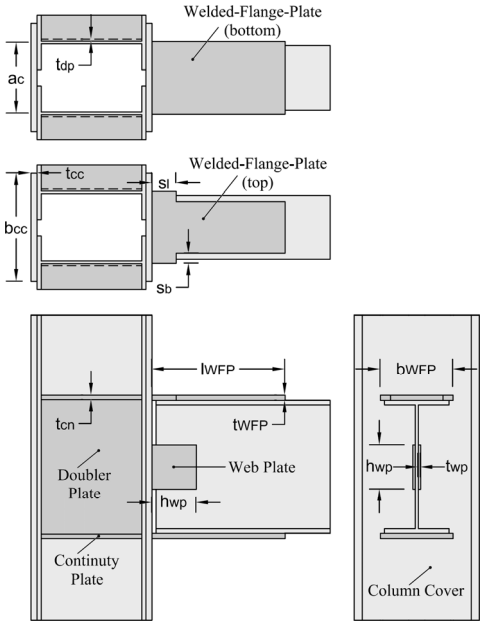

Figure 5: Existing WFP connection details

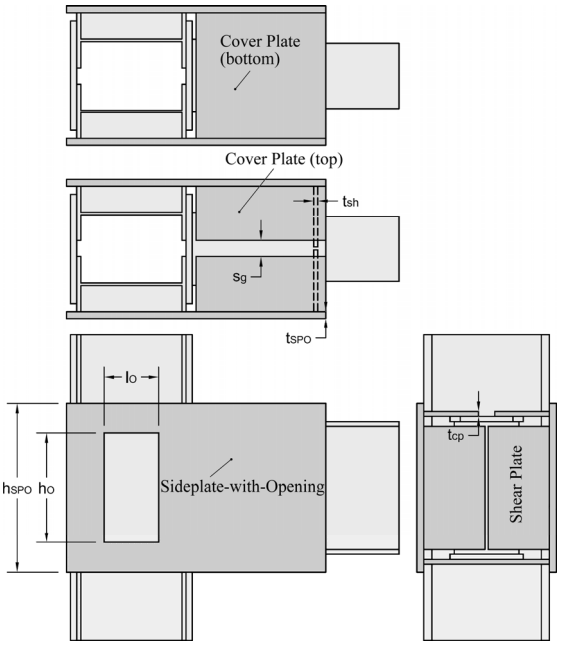

Figure 6: Upgraded SPO connection detail

Table 2: Existing WFP connections detail

Existing Connection	Beam	Column	Welded Flange Plate					Web Plate		Doubler & Continuity Plate	
			l_{WFP}	b_{WFP}	t_{WFP}	s_l	s_b	h_{wp}	t_{wp}	t_{dp}	t_{cn}
WFP-27-16	IPE270	2IPE160	25	16	1.1	6	2.5	9	0.6	0.5	0.8
WFP-27-18	↓	2IPE180	↓	↓	↓	↓	↓	↓	↓	↓	↓
WFP-27-22		2IPE220									
WFP-30-16	IPE300	2IPE160	29	17	1.2			10			1
WFP-30-18	↓	2IPE180	↓	↓	↓			↓			↓
WFP-30-20		2IPE200									
WFP-30-22		2IPE220									
WFP-33-18	IPE330	2IPE180	33	18	1.3			11			1.1
WFP-33-20	↓	2IPE200	↓	↓	↓			↓			↓
WFP-33-22		2IPE220									
WFP-33-24		2IPE240									
WFP-33-27		2IPE270									
WFP-36-22	IPE360	2IPE220	40	19	1.5			12			1.3
WFP-36-24	↓	2IPE240	↓	↓	↓			↓			↓
WFP-36-27		2IPE270									
WFP-36-30		2IPE300									
WFP-36-33		2IPE330									
WFP-40-24	IPE400	2IPE240	44	20	1.6			14			1.4
WFP-40-27	↓	2IPE270	↓	↓	↓			↓			↓
WFP-40-30		2IPE300									
WFP-40-33		2IPE330									

- all dimensions: cm

Table 3: Upgraded SPO connections detail

Upgraded Connection	Existing Connection	Sideplate with Opening				Cover Plate		Shear Plate
		h_{SPO}	t_{SPO}	h_O	l_O	t_{cp}	s_g	t_{sh}
SPO-27-16	WFP-27-16	35	1.5	24	12	1	4	0.8
SPO-27-18	WFP-27-18	↓	↓	↓	↓	↓	↓	↓
SPO-27-22	WFP-27-22							
SPO-30-16	WFP-30-16	38	1.6	24	12	1.1		0.9
SPO-30-18	WFP-30-18	↓	↓	↓	↓	↓		↓
SPO-30-20	WFP-30-20							
SPO-30-22	WFP-30-22							
SPO-33-18	WFP-33-18	42	1.7	27	13.5	1.2		1
SPO-33-20	WFP-33-20	↓	↓	↓	↓	↓		↓
SPO-33-22	WFP-33-22							
SPO-33-24	WFP-33-24							
SPO-33-27	WFP-33-27							
SPO-36-22	WFP-36-22	46	1.8	30	15	1.3		1.1
SPO-36-24	WFP-36-24	↓	↓	↓	↓	↓		↓
SPO-36-27	WFP-36-27							
SPO-36-30	WFP-36-30							
SPO-36-33	WFP-36-33							
SPO-40-24	WFP-40-24	50	2	33	16	1.5		1.2
SPO-40-27	WFP-40-27	↓	↓	↓	↓	↓		↓
SPO-40-30	WFP-40-30							
SPOP-40-33	WFP-40-33							

- all dimensions: cm

3. FINITE ELEMENT MODELING

Typically 20 connections are designed in this study. Only 6 connections with logical distribution on beam and column size are selected for finite element study. Moment-rotation of selected connection and panelzones and rotational capacity of them are extracted using finite element analysis via ANSYS. Selected connections are presented in Table 4.

Table 4: Selected connections for finite element study

Upgraded Connection	Existing Connection
SPO-27-18	WFP-27-18
SPO-27-22	WFP-27-22
SPO-33-22	WFP-33-22
SPO-33-27	WFP-33-27
SPO-40-27	WFP-40-27
SPO-40-33	WFP-40-33

Analysis procedure is according to the qualifying cyclic tests of AISC 341 [2] and FEMA 351 [3]. One-sided subassemblage is used for connection study. It is assumed that the column is pin-supported at mid-story, and the beam is pin-supported at mid-span. Lateral supports were provided to prevent out of plane instability as well as twisting of the beam. A quasi-static cyclic loading history was applied to each specimen. Typical subassemblage model that is used in study is shown in Figure 7.

It is assumed that material property is steel type ST-37. Elastic and inelastic models for ST-37 are used in Finite element modeling. Zones that remain essentially elastic under loading are modeled with elastic material and otherwise with inelastic material. Linear-elastic and trilinear-inelastic material used in modeling are shown in Figure 8.

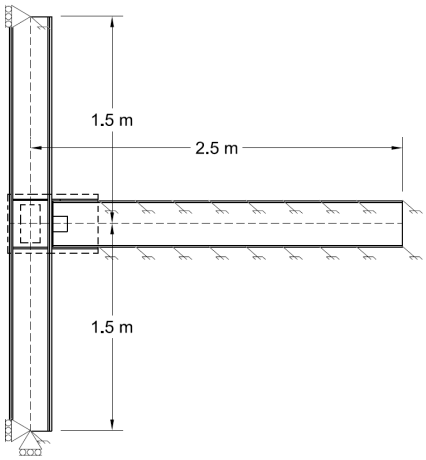

Figure 7: Typical subassemblage model

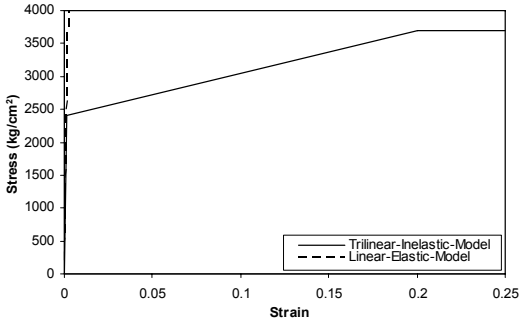

Figure 8: Elastic and inelastic model for material ST-37

Element SOLID45 is used for modeling the specimen's body. Fines mesh is used for Zones that have significant stress distribution. Typical finite element model for existing and upgrade specimens is shown in Figure 9.

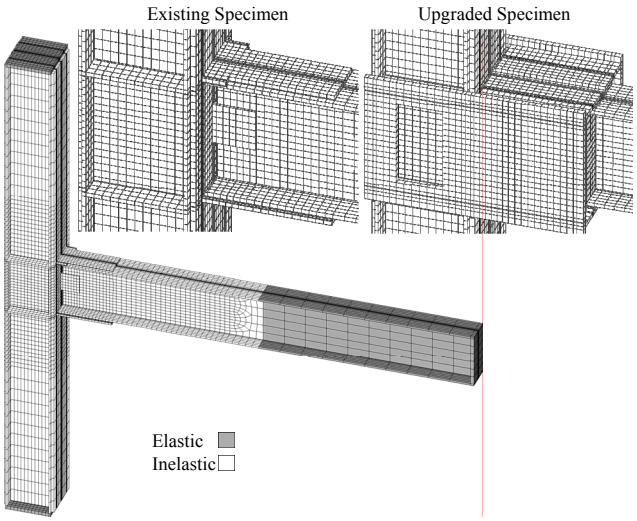

Figure 9: Typical finite element model for specimens

Elements TARGE170 and CONTA173 are used for modeling contact surfaces. Since there is a large proportional deformation between column's cover plate and column's I-section especially in WFP connection, it is necessary to model this surface. Modeling contact surface in column is shown schematically in Figure 10.

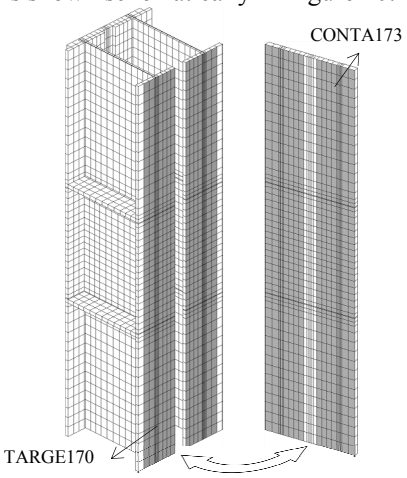

Figure 10: Column's contact surface model

4. VALIDATION

In order to validation, the analytical result must be compared to the experimental result to prove that there is no significant difference between analytical and real response of specimen. Thus, the experimental results of BHRC [4] for common WFP connection in Iran are used.

Specimen S.N.2 is used to validate the results because this specimen is in conformance with the WFP type used in this paper. As mentioned in BHRC [4] this type of WFP connection is commonly used in Iran as a rigid connection. Details of specimen S.N.2 is shown in Figure 11.

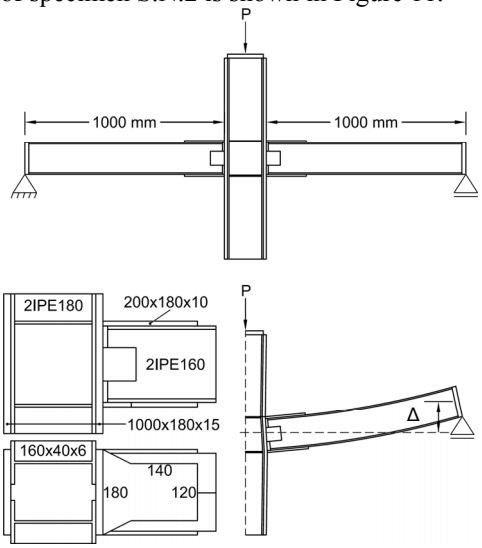

Figure 11: Experimental specimen S.N.2

Finite element Model is constructed according to test setup. Analytical load-displacement curve is compared with experimental shown in Figure 12. As illustrated, there is reasonable conformity among results of analysis and test.

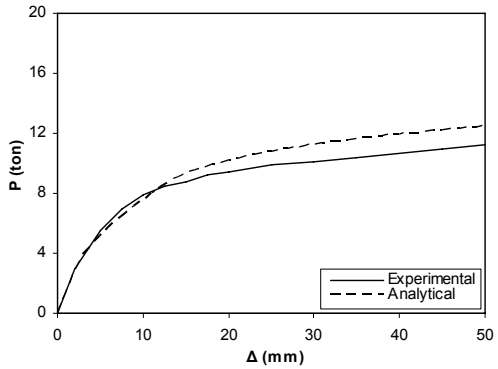

Figure 12: Comparison between analysis and test (S.N.2)

5. Analysis Results

Analysis is performed under standard incremental cyclic loading history on finite element models. FEMA 351 [3] mentioned that cyclic loading must continued until connection failure occurred. According to FEMA 351 [3] interstory drift in failure level is called ultimate drift, θ_U, or collapse prevention drift capacity, θ_{CP}. It is assumed that failure occurred when maximum strain reaches to ultimate strain (assumed 0.2). So analysis continued until maximum strain reaches 0.2. It is assumed that life safety drift capacity, θ_{LS}, is attained from 70% interval of immediate occupancy drift capacity, θ_{IO}, and collapse prevention drift capacity, θ_{CP}.

Panelzone and connection moment-rotation curves are needed for considering these elements in frame analysis. Frame analysis is performed with PERFORM-2D. This computer program capable of considering curves up to trilinear. Therefore, moment-rotation curves must be fitted with consistent multilinear curves. Consequently, panelzones are fitted with linear curves, and existing WFP and Upgraded SPO connections are fitted with trilinear and bilinear curves, respectively.

The equations that are used to calculate the moment-rotation curves from analysis are defined by the following equations and relevant Figure 13.

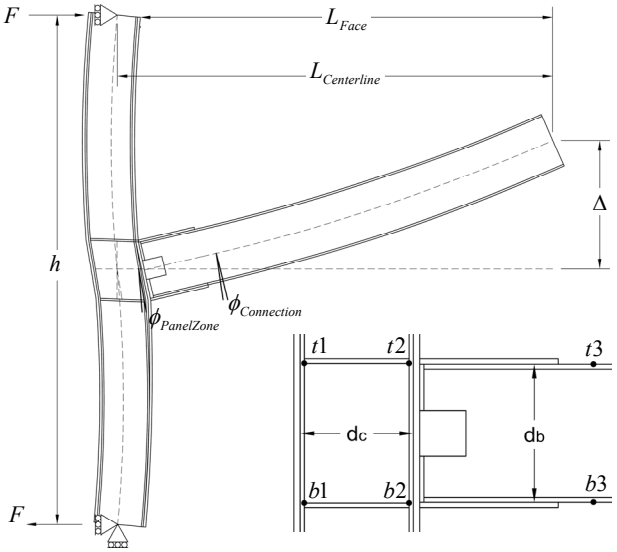

Figure 13: Typical deformed-shaped of specimens

$$M_{Centerline} = F \times h \tag{1}$$

$$M_{Face} = M_{Centerline} \times \frac{L_{Face}}{L_{Centerline}} \tag{2}$$

$$\theta_{InterstoryDrift} = \frac{\Delta}{L_{Centerline}} \tag{3}$$

$$\phi_{PanelZone} = \frac{x_{b1} + x_{b2} - x_{t1} - x_{t2}}{2d_b} + \frac{y_{b1} + y_{b2} - y_{t1} - y_{t2}}{2d_c} \tag{4}$$

$$\phi_{Connection} = \frac{(x_{b3} - x_{b2}) - (x_{t3} - x_{t2})}{d_b} \tag{5}$$

Results for specimens WFP-33-27 and upgraded SPO-33-17 are shown in Figure 14. θ_{IO}, θ_{LS} and θ_{CP} are rotational capacity of connection relevant to Immediate Occupancy, Life Safety and Collapse Prevention performance levels. K_{pz}, panelzone elastic stiffness, K_i and K_h, connection initial and hardening stiffness, M_{fy} and M_{fu}, connection yield and ultimate strength at column face, those obtained through the curve fitting. Finally, results for all selected specimens are presented in Table 5.

Table 5: Analytical results for selected existing and upgraded specimens

Type	Beam-Column (d_b-d_c)	Rotational Capacity			Linear Panelzones	Tilinear WFP/Bilinear SPO Connections			
		θ_{IO} (rad)	θ_{LS} (rad)	θ_{CP} (rad)	K_{pz} (t.m)	M_{fy} (t.m)	M_{fu} (t.m)	K_i (t.m)	K_h (t.m)
WFP	27-18	0.02	0.034	0.04	9677	3.30	6.21	1149.8	88.0
	27-22	0.02	0.041	0.05	13876	3.66	6.54	762.5	67.9
	33-22	0.02	0.027	0.03	16138	5.70	8.81	1540.5	131.0
	33-27	0.02	0.041	0.05	23041	8.60	13.04	1535.7	104.5
	40-27	0.02	0.027	0.03	26930	11.60	16.97	2974.4	222.4
	40-33	0.02	0.041	0.05	39199	16.40	23.12	2688.5	155.5
SPO	27-18	0.02	0.076	0.1	9759	-	13.56	12338.5	-
	27-22	0.02	0.076	0.1	13996	-	13.58	9784.4	-
	33-22	0.02	0.055	0.07	16667	-	23.30	16475.2	-
	33-27	0.02	0.055	0.07	24834	-	23.36	14666.8	-
	40-27	0.02	0.048	0.06	28662	-	39.84	27194.2	-
	40-33	0.02	0.048	0.06	42453	-	39.80	24720.7	-

(a) Connection rotational capacity (b) Linear panelzone model (c) Ttilinear WFP/Bilinear SPO model

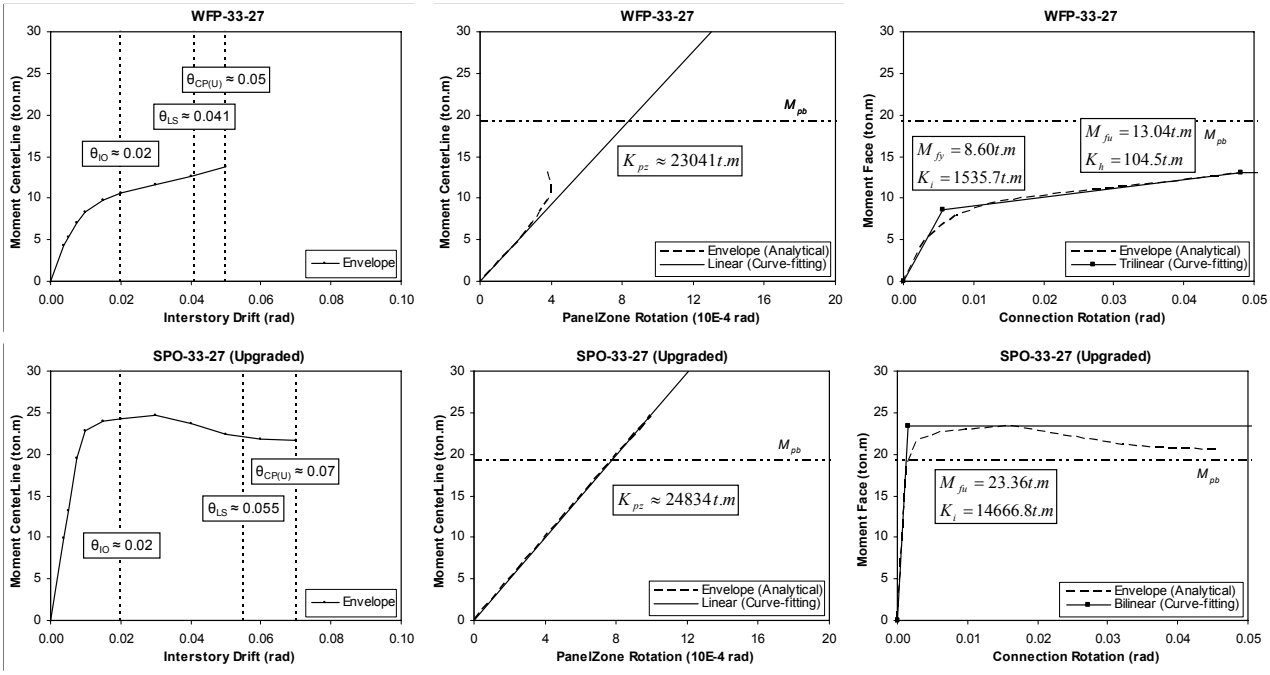

Figure 14: Results for specimens WFP-33-27 and upgraded SPO-33-27

6. PARAMETRIC STUDY

Although the validated computer program may be used to predict the moment–rotation relationship of a connection in lieu of actual test, it is still very time-consuming to use this approach in design practice since one analysis may take dozens of hours to finish on an ordinary PC. Therefore, it is desirable to formulate a mathematical equation represent the moment–rotation relationship for a specific type of connection such as the WFP or upgraded SPO connection considered in this study.

Results for 6 selected connections are fined through the analysis, but the results for all 20 connections in frames are needed for frame analysis. Parametric study is implemented to predict the results of other 14 connection. Using statistical software MINITAB [5] the multiple regression technique is used to formulate prediction equations. Based on parametric study on analytical it is demonstrated that two predictor parameter, depth of beam and column, has the most impact on results. So this parameter are used to predict the response parameters, such as rotational capacity or panelzone or connection moment-rotation characteristic. All prediction equations are in following general form:

$$\left(\theta_{IO}, \theta_{LS}, \theta_{CP} / K_{pz} / M_{fy}, M_{fu}, K_i, K_h\right) = x_1 + x_2 d_b^{\,i} + x_3 d_c^{\,j} \quad (6)$$

x_1, x_2 and x_3 are the coefficients which will be determined through the regression, i and j are the exponents that make best fitting on data.

From statistical measures, namely, the standard error S, the coefficient of determination R^2, and the adjusted coefficient of determination $\overline{R}^2$, lots of information about curve-fitting on results could be attained. The best equations were chosen based on the following three criteria: (1) $R^2, \overline{R}^2 > 90\%$; (2) minimum error S (3) the difference between the predicted value and the calculated value is <10%.

Best fitted equations for response parameters are presented in Table 6. Comparison between analytical results and predicted result are shown in Figure 15. As illustrated, there is good conformity between results of analysis and prediction equations. Results for other 14 connections are predicted by these equations that presented in Table 7.

Table 6: Best fitted equations through the regression

(a) Existing WFP Connection

Response (rad)	Prediction Equation; db, dc (cm)	S	R^2	R^2_{adj}
θ_{IO}	0.02	*	*	*
θ_{LS}	7.33E-2 - 2.00E-3d_b + 4.47E-5d_c^2	0.00154	97.0%	94.9%
θ_{CP}	9.62E-2 - 2.86E-3d_b + 6.39E-5d_c^2	0.00221	97.0%	94.9%
K_{pz}	1.39E+2 + 7.26d_b^2 + 7.65E-1d_c^3	229.736	100.0%	100.0%
M_{fy}	-1.05E-1 + 1.19E-4db^3 + 7.57E-6d_c^4	0.37888	99.7%	99.4%
M_{fu}	1.63 + 1.53E-4d_b^3 + 9.99E-6d_c^4	0.66809	99.4%	99.0%
K_i	1.19E+3 + 1.12E-3d_b^4 - 4.14E+1d_c	124.961	98.8%	97.9%
K_h	2.59E+1 + 4.21E-3d_b^3 - 3.85E-3d_c^3	4.06127	99.7%	99.5%

Table 6: Best fitted equations through the regression (continued)

(b) Upgraded SPO Connection

Response (rad)	Prediction Equation; db, dc (cm)	S	R^2	R^2_{adj}
θ_{IO}	0.02	*	*	*
θ_{LS}	2.73E-1 - 8.70E-3d_b + 1.92E-6d_b^3	0	100.0%	100.0%
θ_{CP}	3.81E-1 - 1.24E-2d_b + 2.74E-6d_b^3	0	100.0%	100.0%
K_{pz}	-8.83E+2 + 7.80db^2 + 8.61E-1d_c^3	191.390	100.0%	100.0%
M_{fu}	1.96E+1 - 1.73d_b + 5.60E-2d_b^2	0.030550	100.0%	100.0%
K_i	1.13E+4 + 4.41E-1d_b^3 - 4.58E+2d_c	529.583	99.7%	99.4%

(a) Existing WFP Connection

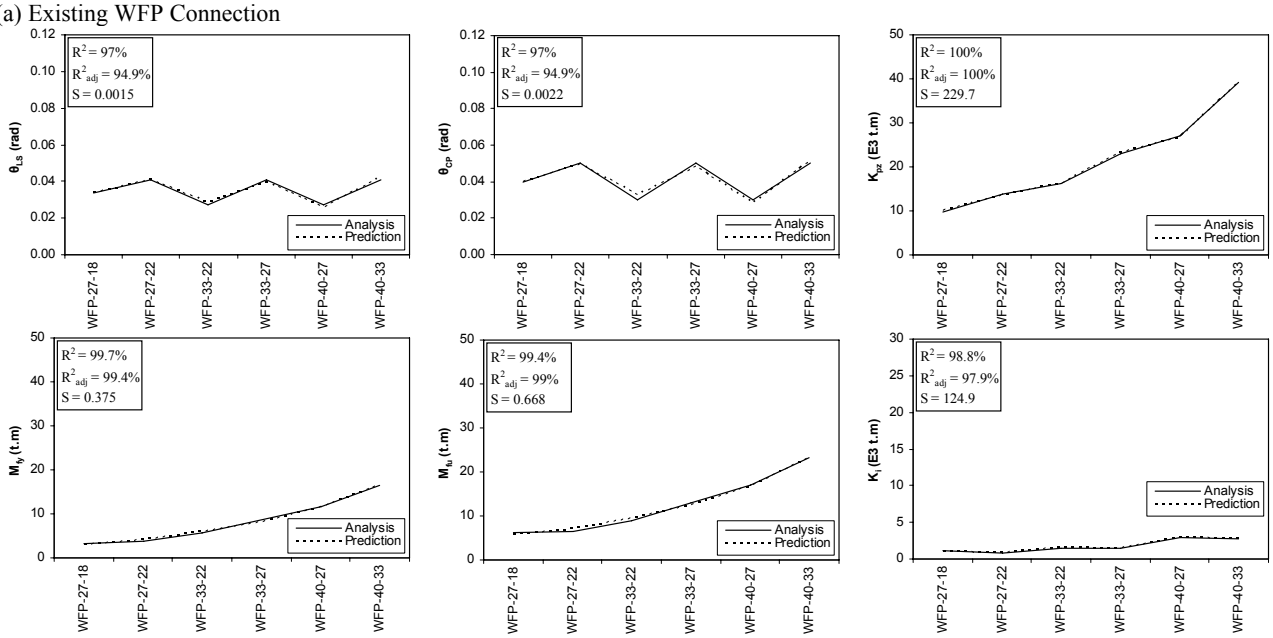

(b) Upgraded SPO Connection

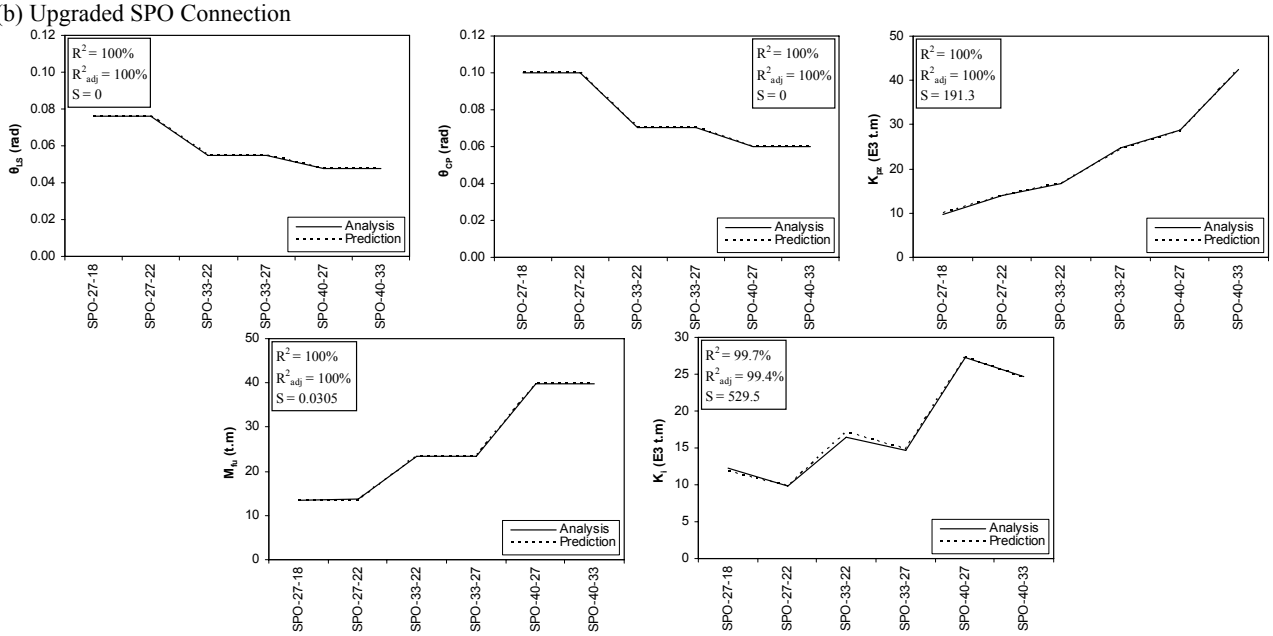

Figure 15: Results for specimens WFP-33-27 and upgraded SPO-33-27

Table 7: Best fitted equations through the regression

(a) Existing WFP Connection

Specimen (db-dc)	θ_{IO} (rad)	θ_{LS} (rad)	θ_{CP} (rad)	K_{pz} (t.m)	M_{fy} (t.m)	M_{fu} (t.m)	K_i (t.m)	K_h (t.m)
WFP-27-16 p	0.02	0.031	0.035	8569	2.74	5.31	1134.8	93.1
WFP-27-18 a	0.02	0.034	0.040	9677	3.30	6.21	1149.8	88.0
WFP-27-22 a	0.02	0.041	0.050	13876	3.66	6.54	762.5	67.9
WFP-30-16 p	0.02	0.025	0.027	9811	3.61	6.43	1448.3	124.0
WFP-30-18 p	0.02	0.028	0.031	11139	3.91	6.82	1365.4	117.3
WFP-30-20 p	0.02	0.031	0.036	12798	4.33	7.37	1282.5	108.9

WFP-30-22 p	0.02	0.035	0.041	14824	4.89	8.11	1199.6	98.7
WFP-33-18 p	0.02	0.022	0.022	12512	4.97	8.19	1788.5	155.0
WFP-33-20 p	0.02	0.025	0.027	14171	5.39	8.74	1705.6	146.6
WFP-33-22 a	0.02	0.027	0.030	16138	5.70	8.81	1540.5	131.0
WFP-33-24 p	0.02	0.033	0.039	18627	6.69	10.46	1539.8	124.1
WFP-33-27 a	0.02	0.041	0.050	23041	8.60	13.04	1535.7	104.5
WFP-36-22 p	0.02	0.023	0.024	17701	7.23	11.13	2178.4	181.6
WFP-36-24 p	0.02	0.027	0.030	20130	7.97	12.10	2095.5	169.3
WFP-36-27 p	0.02	0.034	0.040	24613	9.48	14.10	1971.1	146.7
WFP-36-30 p	0.02	0.041	0.051	30210	11.59	16.88	1846.7	118.5
WFP-36-33 p	0.02	0.050	0.063	37047	14.44	20.64	1722.4	84.1
WFP-40-24 p	0.02	0.020	0.020	22339	10.04	14.76	3086.3	242.4
WFP-40-27 a	0.02	0.027	0.030	26930	11.60	16.97	2974.4	222.4
WFP-40-30 p	0.02	0.033	0.039	32419	13.66	19.54	2837.6	191.6
WFP-40-33 a	0.02	0.041	0.050	39199	16.40	23.12	2688.5	155.5

(b) Upgraded SPO Connection

Specimen (db-dc)	θ_{IO} (rad)	θ_{LS} (rad)	θ_{CP} (rad)	K_{pz} (t.m)	M_{fu} (t.m)	K_i (t.m)
SPO-27-16 p	0.02	0.076	0.100	8340	13.57	12661.4
SPO-27-18 a	0.02	0.076	0.100	9759	13.56	12338.5
SPO-27-22 a	0.02	0.076	0.100	13996	13.58	9784.4
SPO-30-16 p	0.02	0.064	0.083	9675	17.95	15895.0
SPO-30-18 p	0.02	0.064	0.083	11171	17.95	14977.1
SPO-30-20 p	0.02	0.064	0.083	13040	17.95	14059.2
SPO-30-22 p	0.02	0.064	0.083	15323	17.95	13141.3
SPO-33-18 p	0.02	0.055	0.070	12647	23.33	18926.6
SPO-33-20 p	0.02	0.055	0.070	14516	23.33	18008.7
SPO-33-22 a	0.02	0.055	0.070	16667	23.30	16475.2
SPO-33-24 p	0.02	0.055	0.070	19536	23.33	16172.9
SPO-33-27 a	0.02	0.055	0.070	24834	23.36	14666.8
SPO-36-22 p	0.02	0.049	0.062	18415	29.72	21827.7
SPO-36-24 p	0.02	0.049	0.062	21152	29.72	20909.8
SPO-36-27 p	0.02	0.049	0.062	26203	29.72	19533.0
SPO-36-30 p	0.02	0.049	0.062	32510	29.72	18156.1
SPO-36-33 p	0.02	0.049	0.062	40213	29.72	16779.3
SPO-40-24 p	0.02	0.048	0.060	23526	39.82	28574.6
SPO-40-27 a	0.02	0.048	0.060	28662	39.84	27194.2
SPO-40-30 p	0.02	0.048	0.060	34883	39.82	25820.9
SPO-40-33 a	0.02	0.048	0.060	42453	39.80	24720.7

Specimen behavior is founded through the (p): prediction (a): analysis.
Parameters that are founded through analysis underlined.

7. FRAME PERFORMANCE

Frame analysis is carried out by software PERFORM-2D [6]. This software is based on the plastic hinge method and capable of performing nonlinear time history analysis on planer frames. It considers the behavior of beam-to-column connections and panelzones and allows the user to specify moment-rotation of these elements up to trilinear curve. Panelzones are modeled with linear curve, WFP and SPO connections are modeled with trilinear and bilinear curves. Modeling of 3, 7 and 12-story frames are shown schematically in Figure 16.

Frames are analyzed under 7 known earthquake acceleration time history. Maximum story drift during time history is considered for each earthquake. Average story drift for all 7 earthquakes is considered to determine the frame performance level. Earthquakes that are used in study, presented in Table 8.

Performance level of each story is determined by interstory drift to connection rotational capacity ratio. This ratio is called usage ratio. If usage ratio of story is smaller than 1 then it means that story has adequate performance. If all stories satisfy the specific performance level it means that whole frame have that performance level. Finally, calculated story drift and performance level of frames are shown in Figure 17 and percentage of reduction in drift and usage ratios after upgrading connections are shown in Figure 18.

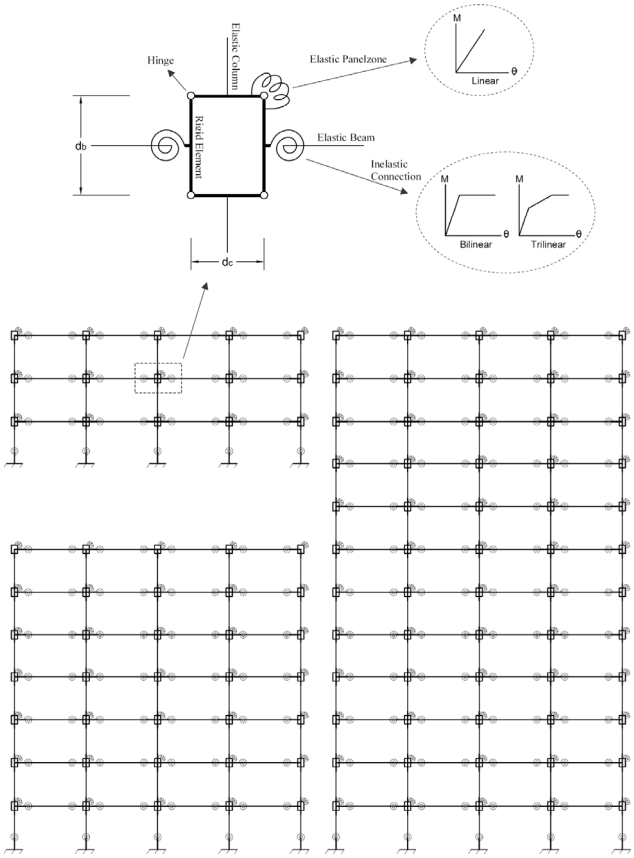

Figure 16: Nonlinear model of frames considering behavior of connections and panelzones

Table 8: Details of earthquakes that are used in study

Earthquake	Bam, Iran 2003	Manjil, Iran 1990	Tabas, Iran 1978	ImperialValley 1979	Kobe, Japan 1995	Loma Prieta 1989	Northridge-01 1994
Station	Bam	BHRC Abbar	9101 Tabas	USGS El Centro	CUE Takarazuka	UCSC 16 LGPC	CDMG Tarzana
PGA (g)	0.7978	0.5051	0.8128	0.5379	0.7069	0.7835	1.6615

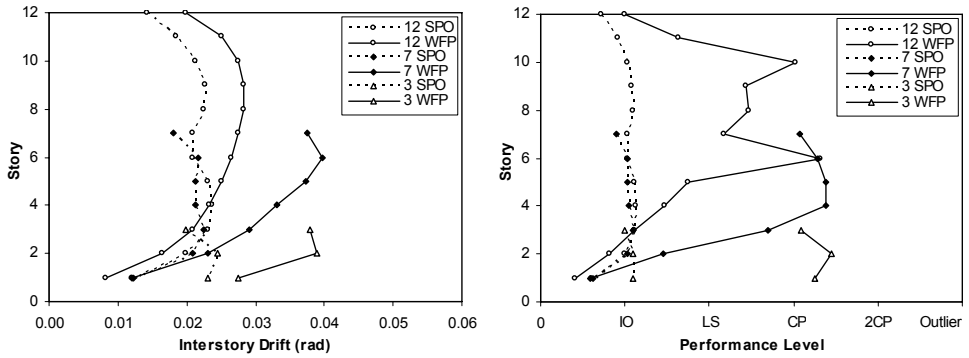

Figure 17: Story drift and performance level of frames (before and after upgrading connections)

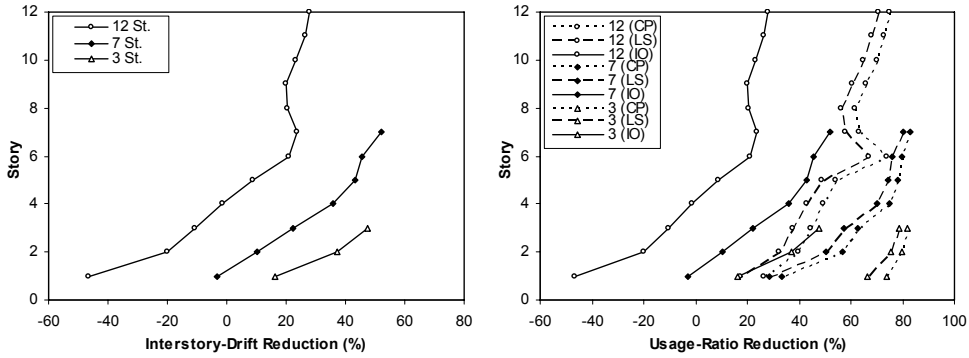

Figure 18: Percentage of reduction in drift and usage ratio after upgrading connections

8. Conclusion

WFP connections with double-I-section column have flexible partially restrained behavior that increase frame deformation. On the other hand, these connections show brittle behavior that decrease the rotational capacity.

Upgrading this common existing connection using Sideplate-with-Opening improves the behavior of connection considerably. Therefore, connection changes to fully rigid and ductile connection that cause to Decrease frame deformation and increase connection's rotational capacity, respectively. Therefore, upgrading this type of common connections can significantly decrease usage ratio and upgrade frame performance level.

Existing frames with WFP connections have not adequate performance level. But these frames are in at least life safety performance level when their connections upgraded with SPO.

Generally, story drift and usage ratio reduce after upgrading connections. This reduction is more significant in lower buildings. Also this reduction is more meaningful in toper stories. Reduction in usage ratio is more impressive in lower performance level (for example, reduction in CP usage ratio is more than IO usage ratio).

9. References

[1] *Iranian Code of Practice for Seismic Resistant Design of Buildings*, Standard No.2800, Building and Housing Research Center, Tehran, Iran, 1999.

[2] AISC/ANSI 341-05; *Seismic Provisions for Structural Steel Buildings*, American Institute of Steel Construction, Inc., Chicago, IL, 2005.

[3] FEMA 351; *Recommended Seismic Evaluation and Upgrade Criteria for Existing Welded Steel Moment-Frame Buildings*, Federal Emergency Management Agency, Washington, DC, 2000.

[4] A. Mazrooe, W. Simonian and M. Nikkhah Eshghi, "Experimental Evaluation of Rigid Welded Connections Used in IRAN", Building and Housing Research Center, Tehran, Iran, 2005.

[5] Minitab. MINITAB Release 14.2, http://www.minitab.com; 2005.

[6] Graham H. Powell Inc. "Ram Perform-2D Basic Tutorial", January 2001.